Journal of Sound and Vibration (1998) **217**(3), 485–505
Article No. sv981767

THE ENHANCEMENT OF IMPULSIVE NOISE AND VIBRATION SIGNALS FOR FAULT DETECTION IN ROTATING AND RECIPROCATING MACHINERY

S. K. Lee and P. R. White

Institute of Sound and Vibration Research, *University of Southampton*, *Highfield*, *Southampton S*017 1*BJ*, *England*

(*Received* 15 *April* 1997, *and in final form* 26 *May* 1998)

Impulsive sound and vibration signals in machinery are often caused by the impacting of components and are commonly associated with faults. It has long been recognized that these signals can be gainfully used for fault detection. However, it tends to be difficult to make objective measurements of impulsive signals because of the high levels of background noise. This paper presents an enhancement scheme to aid the measurement and characterization of such impulsive sounds, called a two-stage Adaptive Line Enhancer (ALE), which exploits two adaptive filter structures in series. The resulting enhanced signals are analyzed in the time–frequency domain to obtain simultaneous spectral and temporal information. In order to apply the two-stage ALE successfully the filter parameters and adaptive algorithms should be chosen carefully. Conditions for the choice of these parameters are presented and suggestions are made for suitable adaptive algorithms. Finally, the techniques developed are applied to the diagnosis of faults within an internal combustion engine and to data from an industrial gearbox.

© 1998 Academic Press

1. INTRODUCTION

The use of acoustic and vibration measurements for the purposes of machine condition monitoring is an established field [1]. The signals measured from machinery in a normal condition are commonly complicated signals containing both narrowband and broadband components. The presence of a fault is often indicated by the presence, or increase in, impulsive signal elements [1, 2]. These impulsive signals may be due to a change of stiffness or mass in the system [3, 4] and by characterizing them one can gain insight into the likely causes of the fault. The detection of these impulsive signals is hampered by the presence of the signals associated with the normal running of the machine, with the consequence that the detection of the weak impulsive signals, which are especially associated with incipient faults, is difficult. It is the 'normal' signals which form the background noise environment against which the detection of fault induced impulsive signals must be conducted. To aid fault detection, it is valuable to enhance the impulsive

0022–460X/98/430485 + 21 $30.00/0 © 1998 Academic Press

signals by suppressing this background noise prior to further processing. Such pre-processing can be based upon one of several signal processing paradigms. After successful pre-processing the signal has an increased Signal to Noise Ratio (SNR), which makes it more amenable to one of a gamut of signal processing tools which can be used to characterize the signal, including Auto-Regressive (AR) modelling [5], kurtosis evaluation [6], cepstrum analysis [7], time–frequency analysis [8–10], higher order spectra [11] and higher time frequency analsis [12].

This paper is concentrated on the problem of pre-processing the measured signals to permit a more accurate characterization of the fault related impulsive components. Several such schemes have been proposed, but the most prevalent of these is time domain averaging [2, 13, 14]. This involves averaging data from successive cycles of the machine component being studied. To use time domain averaging one requires information about the rotation speed of a machine, usually supplied in the form of synchronized pulse signals. With access to a reliable synchronized signal, time domain averaging represents one form of coherent averaging, which is an optimal method for the reduction of random noise components. Time domain averaging, with suitable implementation, can also cope with non-stationary situations where the rotation speed is varying. The consequence of this is that time domain averaging is a widely used, and powerful, pre-processing tool. However, it can be inefficient at reducing some tonal components of the background noise: i.e., those that are commensurate (or nearly commensurate) with the rotational frequency. The result of this is that the time averaged signal may possess so-called 'ghost components' [4, 8], which are residual narrowband signals that time domain averaging is poor at attenuating. There are also some applications in which a synchronization signal is either unavailable or is of poor quality. In this paper a pre-processing scheme is considered which addresses problems in which suitable synchronizing information is unavailable; the scheme also avoids the generation of ghost components.

One pre-processing method which does not rely upon synchronization, is based on the Adaptive Noise Canceller (ANC) [17]. Whilst this method does not require a signal synchronized to the shaft rotation it does need a second, reference, measurement, which is correlated only with either the background noise or the impulsive signals. Again there are applications where such a reference signal is not readily available.

In this paper an enhancement scheme is developed, referred to as a two-stage ALE (Adaptive Line Enhancer), specifically for situations where no synchronous or reference signal is available. The first stage of the scheme is employed to remove the tonal signal components of the background noise, whilst the second stage is aimed at enhancing the impulsive signal relative to the broadband random components. Successful application of the algorithm depends on careful selection of the parameters of the adaptive filters at each stage. Conditions are developed and presented for the selection of these parameters; choices are proffered for the update algorithms in the adaptive filters. Specifically, the LMS algorithm is used for the first stage and the QR-LSL algorithm (a least squares lattice algorithm based on QR decomposition) is employed for the second. To illustrate the effectiveness of the scheme, the output is examined via its time–frequency

representation. A model of the noise/vibration signals is presented, reflecting an archetypal acoustic or vibration signal measured in such problems. These model signals are then processed by using the proposed strategy. Beyond these simulation examples, results are also presented for data measured from real systems, specifically from an automotive engine and an industrial gearbox.

2. ADAPTIVE SIGNAL PROCESSING

2.1. ADAPTIVE NOISE CANCELLATION (ANC)

Classical adaptive filters are linear (normally FIR) digital filters which adjust their parameters (coefficients) in order to optimize some performance criterion. Figure 1(a) depicts such a structure configured in a noise cancelling mode, as discussed in reference [17]. In this mode the adaptive filter requires two inputs; the desired signal, d_k, and a reference measurement x_k.

For the sake of this discussion it is assumed that the desired input to the filter consists of measurements of a signal of interest, s_k, corrupted by an additive noise, w_k: i.e., $d_k = s_k + w_k$. For successful operation of the filter the reference signal, x_k, should be an independent measurement of the corrupting noise and be uncorrelated with the signal of interest. The filter automatically adjusts its coefficients in such a way as to minimize some cost function, normally the mean squared error, $E[e_k^2]$. By filtering x_k one can construct an estimate of the corrupting noise signal, w_k, but one cannot form an estimate of s_k, since it is assumed that x_k and s_k are uncorrelated. By minimizing the mean squared error one forces the filter output, y_k, to become an estimate, w_k, which when subtracted from d_k yields an enhanced version of s_k.

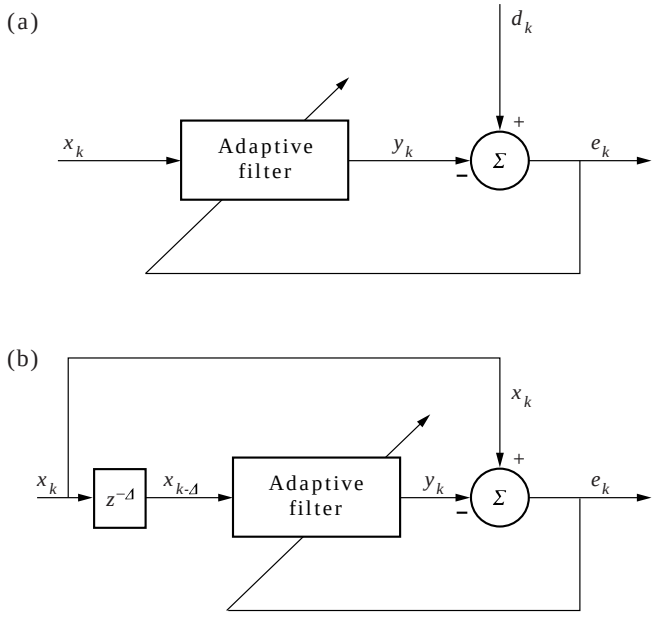

Figure 1. Adaptive filter configurations: (a) adaptive noise canceller; (b) adaptive line enhancer.

The problem with ANC is that one requires a reference signal which is strongly correlated with the noise signal, w_k, but uncorrelated with the signal of interest. The performance of an ANC scheme is usually limited by the availability and quality of the reference signal.

2.2. ADAPTIVE LINE ENHANCEMENT

An alternative mode of operation for an adaptive filter, based on ANC, is provided by an adaptive line enhancer (ALE), as shown in Figure 1(b). This is a simple variation on the ANC requiring only a single input signal. In this case the reference signal is obtained by delaying the input signal by a fixed number of samples, Δ. The adaptive filter then endeavours to predict the signal x_k from the delayed samples. The result is that any input components which are predictable over the delay appear at the filter output, y_k, whilst the error signal, ε_k, contains those components which are unpredictable over the delay. The classical application of this technique is to enhance narrowband signals in noise, in applications such as SONAR.

It should be noted that the filter offers estimates of both the broadband and narrowband signals so can be used equally for the suppression of tonal signals.

2.3. ADAPTIVE FILTER ALGORITHMS

There exists a vast array of algorithms for updating the coefficients of the adaptive filter (see, e.g., references [19, 22]). The most commonly considered is the Least Mean Squares (LMS) algorithm, whose update equation is $\mathbf{w}_{k+1} = \mathbf{w}_k + \mu\varepsilon_k\mathbf{w}_k$, where $\mathbf{w}_k$ is a vector containing the L coefficients of the FIR filter, $\mathbf{x}_k$ is a vector containing the L most recent samples of the reference time series and μ is a user-defined constant which determines the convergence characteristics of the filter.

The LMS algorithm is the basis of most adaptive filters used in practice. The primary reason for this is the LMS's simplicity. Specifically it has a computational load which is proportional to the filter length, making it realizable in many real-time applications. However whilst the LMS algorithm has great practical utility it does suffer from performance limitations which stem from the competing requirements faced when choosing μ. Large values of μ are needed for rapid convergence but these large values also induce a large steady state error in the converged filter, termed misadjustment.

An alternative class of adaptive filter algorithms is based on the concept of least squares. These algorithms exactly optimize a data dependent criterion. Within the class of least squares methods there are a great many algorithms one can select from and it should be emphasized that these methods compute (in theory) the same solution and hence have the same performance. The class of least squares algorithms have the advantage of rapid transient convergence, i.e., their initial convergence, and adaptation to abrupt changes in a signal, is superior to that of the LMS.

Original formulations of the least squares algorithms required a computational load proportional to L^2, which generally rendered them impractical for real time implementation. Later formulations appeared which compute the least squares

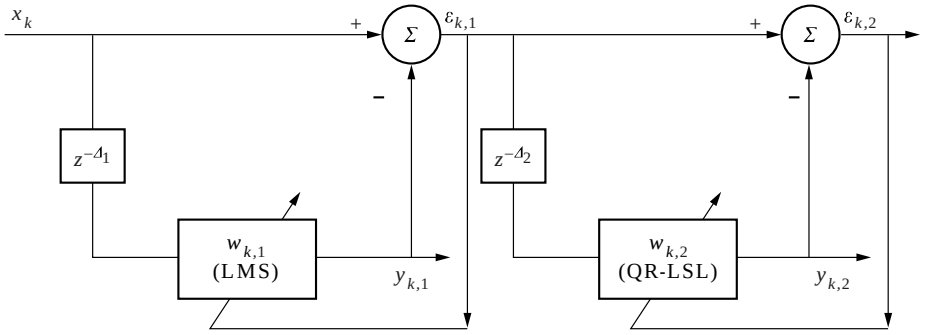

Figure 2. Two-stage ALE.

solution requiring a computational load which is proportional to L. These 'fast' formulations suffer severely from numerical instabilities, with the result that after a relatively small number of iterations the algorithms diverge. More recently, alternative fast formulations with much greater nunerical stability have been proposed: e.g., the QR lattice [19, 23]. These algorithms are significantly more computationally intensive than LMS but they are practical for small filter lengths and have significant performance advantages over the LMS algorithm.

2.4. A TWO-STAGE ALE FOR ENHANCEMENT OF IMPULSIVE SIGNALS

The purpose of this section is to discuss adaptive methods for enhancing impulsive signals which are masked by both broadband random noise and narrowband tonal signals. The proposed solution is based upon a two-stage ALE [18], a block diagram of which is shown in Figure 2. This structure consists of two ALE applied in series, each aiming to achieve distinct goals. The first stage aims to remove the tonal noise components, whilst it is the task of the second stage to reduce the broadband noise.

In this configuration the error signal from the first ALE is passed to a second stage of processing. The notation is modified to distinguish between signals in the two stages; see Figure 2 for details. Specifically the error signal, $\varepsilon_{k,1}$, is used as the input signal to the second ALE. The function of the second stage is to enhance the impulsive signals relative to the broadband noise. The philosophy here relies on the assumption that impulsive signals are locally predictable: i.e., that they can be thought of as relatively narrowband transient events. The impulses are clearly non-stationary, but if the adaptive filter is agile enough, it is able to successfully perform local predictions on the impulsive signals. In this way one can obtain enhancements of such signals relative to the broadband noise. The delay Δ_2 must be selected to be short enough to ensure that the impulsive signals do not decorrelate, but sufficiently large as to decorrelate the noise. The choice $\Delta_2 = 1$ is a conservative one, since it minimizes the attenuation of impulsive signals, but in choosing it one assumes that the background noise has a flat spectrum. It is this option which is employed in this paper. The final output of the two-stage ALE system is the filter output $y_{k,2}$.

2.5. SELECTION OF THE ADAPTIVE ALGORITHMS

It is important to determine which type of adaptive algorithm should be used in each of the two stages of this scheme. The objective of the first stage ALE is to remove the harmonic components from the input signal. To achieve this successfully a long filter length is required to increase the attenuation of the filter at the harmonic frequencies and also to remove the interactions between the various spectral lines [20]. The LMS algorithm [19] is suited for this task because of its relatively low computational cost when long filter lengths are employed. The objective of the second stage ALE is to reduce the level of the broadband noise. The impulsive signals are cyclic with a short duration and are non-stationary. The adaptive algorithm must have rapid transient convergence characteristics to track these non-stationarities. To achieve the required rapid convergence, an exact least squares algorithm [18, 21, 22] is recommended. To keep the computational load as small as possible one is naturally drawn to the 'fast' formulations of these algorithms, such as the QR lattice algorithm.

2.6. DETERMINATION OF FILTER LENGTH

The periodic nature of the impulsive signal lays open the possibility that the first stage of the scheme will identify them with the narrowband components and in doing so attenuate them. To avoid such an eventuality care over the choice of the parameters Δ_1 and L_1 must be exercised. For the LMS algorithm the update equation for the filter weight vector $\mathbf{w}_k$ can be written as

$$\mathbf{w}_{k+1} = (I - \mu \mathbf{x}_{k-\Delta_1} \mathbf{x}_{k-\Delta_1}^{\mathrm{t}}) \mathbf{w}_k + \mu x_k \mathbf{x}_{k-\Delta_1}. \tag{1}$$

From equation (1), with $\mathbf{w}_0 = 0$, it is noted that if for all k either x_k or $\mathbf{x}_{k-\Delta_1}$ is zero, the weight vector remains zero. For the impulsive signal shown in Figure 3(a) this condition is met when $L_1 < T_\mathrm{p} - 2\Delta_1$, where T_p is the period of the signal. Under this assumption, (1) when $0 \leqslant k \leqslant \Delta_1$,

$$x_k \neq 0, \qquad \mathbf{x}_{k-\Delta_1} = \mathbf{0}, \tag{2}$$

and (2) when $\Delta_1 < k < T_\mathrm{p}$,

$$x_k = 0, \qquad \mathbf{x}_{k-\Delta_1} \neq \mathbf{0}, \tag{3}$$

Hence, if the condition $L_1 < T_\mathrm{p} - 2\Delta_1$ is satisfied, then the filter's coefficients remain at zero and the impulsive signal is not attenuated by the adaptive filter, as shown in Figures 3(c) and (d), whereas $\mathbf{w}_k$ is non-zero if the condition $L_1 < T_\mathrm{p} - 2\Delta_1$ is not satisfied. A similar effect can be noted in the presence of broadband noise as shown in Figures 3(e) and (f). In this case the coefficients of the adaptive filter are non-zero because of a low level of noise corruption. From a statistical viewpoint, by taking the expectation of equation (1) one obtains (assuming the statistical independence of $\mathbf{x}_{k-\Delta_1}$ and $\mathbf{w}_k$)

$$\mathrm{E}[\mathbf{w}_{k+1}] = (I - \mu \mathrm{E}[\mathbf{x}_{k-\Delta_1} \mathbf{x}_{k-\Delta_1}^{\mathrm{t}}]) \mathrm{E}[\mathbf{w}_k] + \mu \mathrm{E}[x_k \mathbf{x}_{k-\Delta_1}]. \tag{4}$$

Equation (4) illustrates that under the previous assumptions then $E[\mathbf{w}_k] = 0$, since $E[x_k \mathbf{x}_{k-\Delta_1}] = 0$, and $\mathbf{w}_0 = \mathbf{0}$. Further assuming a slow adaptation rate also means that the level of misadjustment will be small, implying that $\mathbf{w}_k \approx \mathbf{0}$ [19]. The above restriction on the length of the filter is at odds with the desire to increase resolution, and hence increase the attenuation of the unwanted narrowband

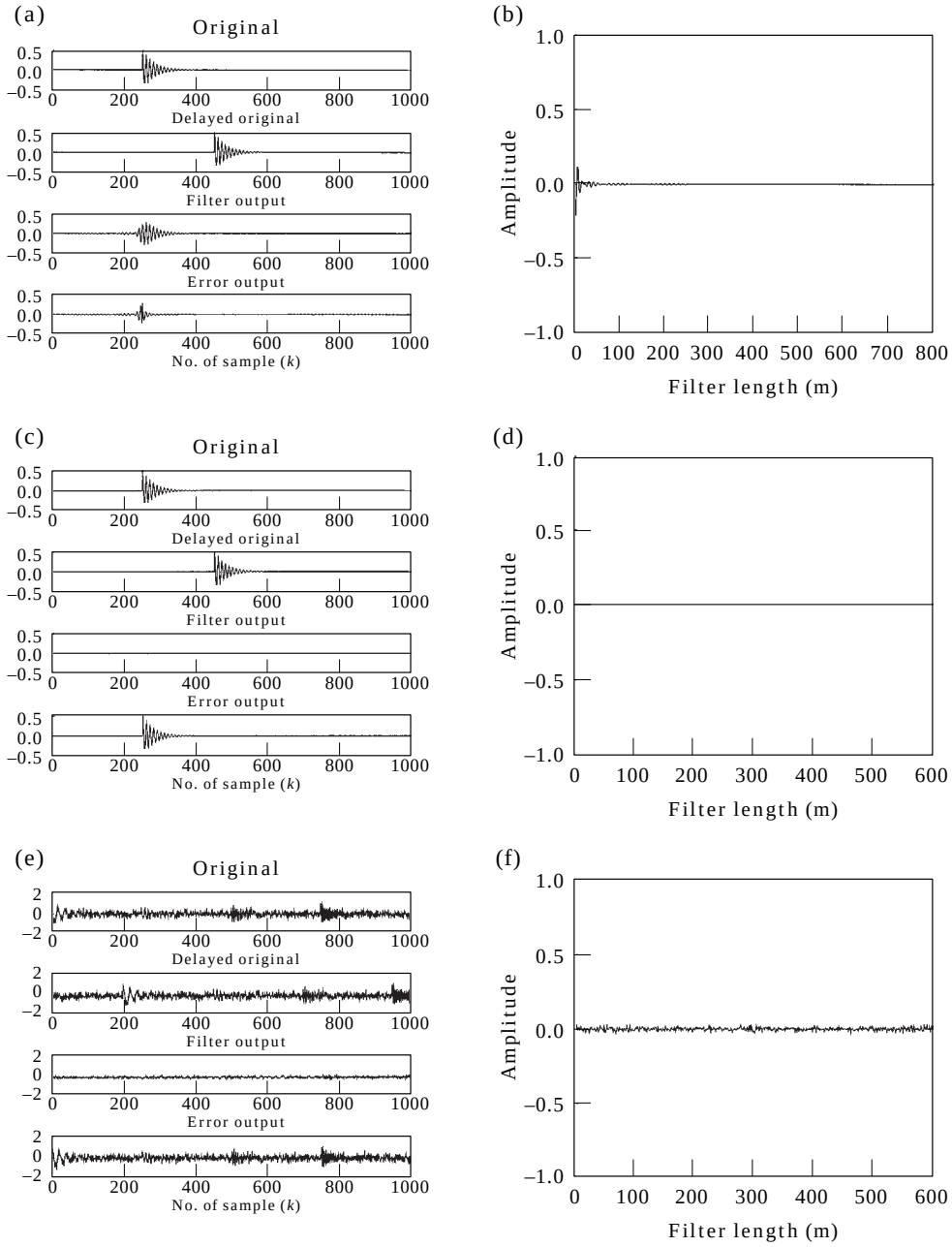

Figure 3. (a) Noise-free signal, $L_1 > T_p - 2\Delta_1$; (b) impulse response of the adaptive filter; (c) noise-free signal, $L_1 < T_p - 2\Delta_1$; (d) impulse response of the adaptive filter; (e) additive Gaussian noise; (f) impulse response of the adaptive filter.

signals. One aims to select L_1 as close to $T_p - 2\Delta_1$ without exceeding it (note that T_p is generally not known *a priori*).

3. TIME–FREQUENCY ANALYSIS

Having applied the two-stage pre-processing scheme one is still left with the problem of characterizing the signals. Herein this characterization will be performed via a time–frequency representation. Such a characterization allows information about the temporal location and frequency content of a fault signal to be identified simultaneously.

There is a wide variety of time–frequency analysis techniques available. Within this paper attention is restricted to the so-called bilinear class of distributions. These have the advantage that they can be easily constrained to yield real distributions which can be interpreted as two dimensional decompositions of a signal's energy. Mathematically, a generalized bilinear time–frequency representation is described as a member of Cohen's class [24] and can be written in the form

$$S(t,f) = \int_{-\infty}^{\infty}\int_{-\infty}^{\infty} \phi(u-t,\tau)x\left(u+\frac{\tau}{2}\right)x^*\left(u-\frac{\tau}{2}\right)\mathrm{e}^{-\mathrm{j}2\pi f\tau}\,\mathrm{d}u\,\mathrm{d}\tau, \tag{5}$$

where $\phi(t,\tau)$ is the kernel function which distinguishes one member of Cohen's class from another. If the kernel function is selected such that $\phi(t,\tau) = \delta(t)$ for all τ, where $\delta(t)$ is the Dirac delta function, equation (5) reduces to the well-known Wigner distribution. It is interesting to note that for this kernel the temporal resolution is as sharp as possible, because of the Dirac impulse, whilst the frequency resolution is related only to the duration of the signal record available. Thus, generally, the Wigner distribution has good time–frequency resolution. However, it has unwanted properties, such as the fact that it can be negative and that it contains interference terms between components. In order to smooth these cross-terms, a variety of methods has been proposed. Conventionally this work has been concentrated on the problem of determining suitable kernel functions, $\phi(t,\tau)$ [24], which retain the desirable properties of the Wigner distributions but mitigate some of its less desirable characteristics. In this paper one commonly considered kernel function introduced by Choi and Williams [25] is employed which has an exponential form, and leads to a representation

$$W(t,f) = \int_{\tau} \mathrm{e}^{-\mathrm{j}2\pi f\tau}\int_{u}\frac{1}{2\tau}\sqrt{\frac{\upsilon}{\pi}}\,\mathrm{e}^{-\mathrm{j}2\pi(f\tau+\upsilon(u-t)^2/4\tau^2)}x\left(u+\frac{\tau}{2}\right)x^*\left(u-\frac{\tau}{2}\right)\mathrm{d}u\,\mathrm{d}\tau, \tag{6}$$

where υ ($\upsilon > 0$) is a scaling factor and controls the kernel shape.

4. NUMERICAL MODELS FOR NOISE/VIBRATION SIGNALS

4.1. GENERAL SIGNAL MODEL STRUCTURE

The form of signals encountered in the condition monitoring applications considered here is complicated, containing several different classes of signal components. In this section a general signal model is presented which is aimed at encapsulating the essential elements of signals from both a reciprocating engine and a gearbox. The model employed can be expressed as

$$x(t) = s_{\mathrm{h}}(t) + s_{\mathrm{i}}(t) + i(t) + n(t), \tag{7}$$

where $s_{\mathrm{h}}(t)$ represents harmonic narrowband signal components, i.e., tonal signals at frequencies which are integer multiples of the fundamental rotation speed, $s_{\mathrm{i}}(t)$ is the sum of the incommensurate narrowband components, i.e., non-harmonically related tonal signals, $i(t)$ is the impulsive signal which represents the signal to be enhanced via this pre-processing scheme and finally $n(t)$ is a broadband random noise, in this case modelled as Gaussian white noise.

4.2. SIGNAL MODEL OF AUTOMOTIVE ENGINE DATA

In using equation (7) to model acoustic data from a car engine one can identify the various model elements with physical mechanisms. The harmonic signals relate to combustion and mechanical noise, the frequency content of which is modified by the transmission path through which these signals are measured. The non-harmonic components can arise from belt-driven components, such as the alternator and cooling fan, whilst the broadband signal components arise from a range of sources such as aerodynamic noise from the fan and airflow at the intake/exhaust. Finally, the impulsive, fault related, signal can also be generated via a number of mechanisms including combustion knocking and worn components.

One period of the signal used to model noise from an automotive engine is shown in Figure 4(e). This signal is based on equation (7), with its Fourier transform depicted in Figure 4(f). The high amplitude wave, of which one period can be seen, is the harmonic signal $s_{\mathrm{h}}(t)$ and is shown in Figure 4(a). Figure 4(b) depicts the impulsive component, $i(t)$ which contains four distinct components (nominally one per cylinder) whose centre frequencies are 0·5 kHz, 1·5 kHz, 2·0 kHz and 3·0 kHz. These impulses are modelled as exponentially decaying sine waves. There are two non-harmonic components making up $s_{\mathrm{i}}(t)$, shown in Figure 4(c). The frequencies of these tones are 2·5 kHz and 0·9 kHz. Figure 4(d) shows the broadband noise signal $n(t)$.

4.3. SIGNAL MODEL OF GEARBOX VIBRATION DATA

The model (7) can be used to simulate vibration data from a gearbox. In the case of gearbox data many of the signal components are generated via amplitude or phase/frequency modulations and as a consequence the signal model (7), being additive in nature, would appear to be inappropriate. However the harmonic component, $s_{\mathrm{h}}(t)$, upon assuming both the carrier and modulation signals to be harmonic with the shaft rotation, can be expressed in a Fourier series form and

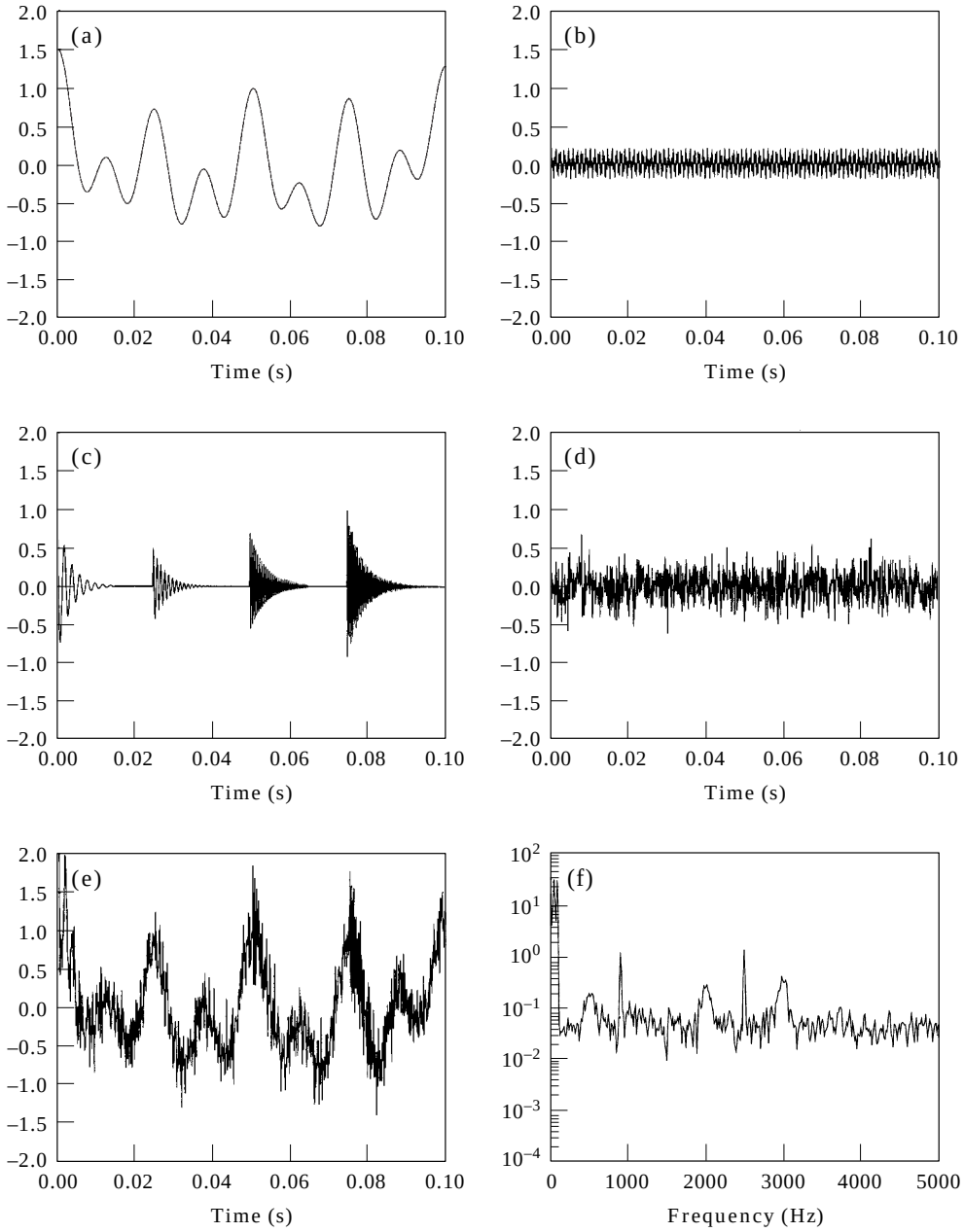

Figure 4. The model signal of noise from an internal combustion engine. (a) fundamental firing frequency and harmonics of crankshaft rotation speed; (b) pure tone noise at 0·9 kHz and 2·5 kHz; (c) four multiple impulsive sounds at 0·5 kHz, 1 kHz, 2·0 kHz, 3 kHz; (d) broadband Gaussian noise; (e) one period of the signal model; (f) Fourier transform of signal model.

so be represented as the sum of harmonic components. Further, in the case of small magnitude phase modulations an additive model is reasonable [16]. In the terminology of this application one considers the signal to consist of two elements, the so-called regular and residual signals [16], the regular signals being the

harmonic components, $s_h(t)$, and the residual signal being the difference between the complete signal and the harmonic term: i.e., $s_i(t) + n(t) + i(t)$.

The synthetic signal for the vibration data from a gearbox is shown in the time domain in Figure 5(e), with its Fourier representation in Figure 5(f). The tooth-meshing frequency is assumed to be 80 Hz. Figure 5(a) shows the pure tone

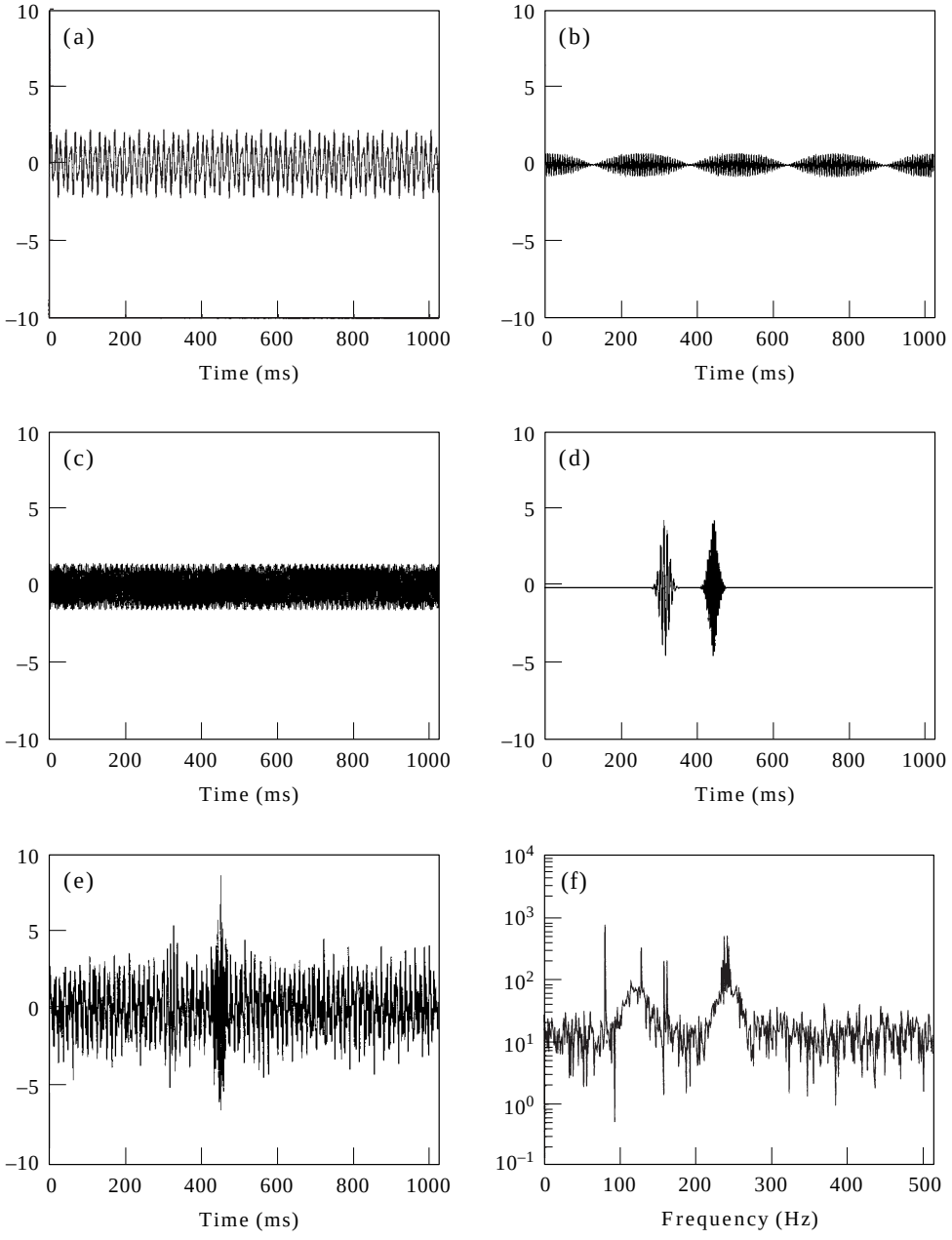

Figure 5. The signal model for gear fault. (a) Regular signal $x_b(t)$; (b) amplitude modulated component; (c) phase modulated component; (d) impulsive signal; (e) total signal model; (f) Fourier transform of signal model.

TABLE 1

Parameters used for the two-stage ALE

	First stage ALE	Second stage ALE
Filter length (L)	600	8
Decorrelation delay (Δ)	200 (20 ms)	1 (0·1 ms)
Convergence step-size (μ)	$0{\cdot}2/\lambda_{max}$	
Forgetting factor (λ)		0·96
Period length	1000 (100 ms)	1000

signals, one at the fundamental frequency 80 Hz and the second, representing a ghost component, at 128 Hz. There is also an amplitude modulated signal, as shown in Figure 5(b). This is formed by multiplying a 160 Hz (the second order meshing frequency) sine wave by a 2 Hz sine wave. Figure 5(c) shows a phase modulated signal consisting of a carrier signal with a centre frequency of 240 Hz (the third order meshing frequency), phase modulated by a 2 Hz sine wave. There are two impulsive signals per revolution, displayed in Figure 5(d). One is a windowed 120 Hz sine wave, where a short duration Hanning window is chosen as the amplitude modulation function. The other impulse is modelled by a windowed chirped sine wave, $\sin(2\pi 240t + \sin(2\pi 2t))$, where the windowing function is the same as that used for the first impulse.

4.4. APPLICATION OF TWO-STAGE ALE TO THE MODELLED IMPULSIVE SIGNALS

In the previous two sections signal models aimed at typifying the acoustic and vibration signals encountered in rotating machinery have been discussed. Within these signals the detection of impulsive components is made difficult by the additional noise components and conventional spectral analysis methods, based on the FFT, fail. In this section the results of applying adaptive techniques to this simulated data are presented.

The parameters of the adaptive schemes are selected in accordance with the design criteria discussed earlier. The adaptation constant, μ, for the first stage is selected as $\mu = 0{\cdot}2/\lambda_{max}$ (where λ_{max} is the largest eigenvalue of the input auto-correlation matrix). The delay has to be sufficiently long so as to decorrelate the impulses, and this can be achieved by making the delay at least the duration of each impulse, in this example $\Delta_1 = 200$ (20 ms). The filter length must also satisfy $L_1 < T_p - 2\Delta_1$ which is achieved here by selecting $L_1 = 600$. Information about a suitable choice of the second filter length L_2 can be made by plotting the minimum mean squared error against the weight vector length [28] or alternatively by the use of Singular Value Decomposition [29]. To ensure that the filter is capable of rapid adaptation then short filter lengths should be employed; in this simulation $L_2 = 8$ was selected. The delay Δ_2 was set to one sample for reasons already discussed. The convergence of the exact least squares algorithms is controlled via a parameter called the forgetting factor, λ, which has an equivalence to $1–2\mu$, where μ is the convergence coefficient in the LMS algorithm. Usually λ

is selected such that $0{\cdot}9 < \lambda < 0{\cdot}99$; here we use $\lambda = 0{\cdot}96$. Table 1 summarizes all the parameter choices employed in the adaptive schemes used herein.

The result of applying the two-stage ALE to the synthetic engine data signal is depicted in Figure 6. The impulsive components are difficult to discern in the

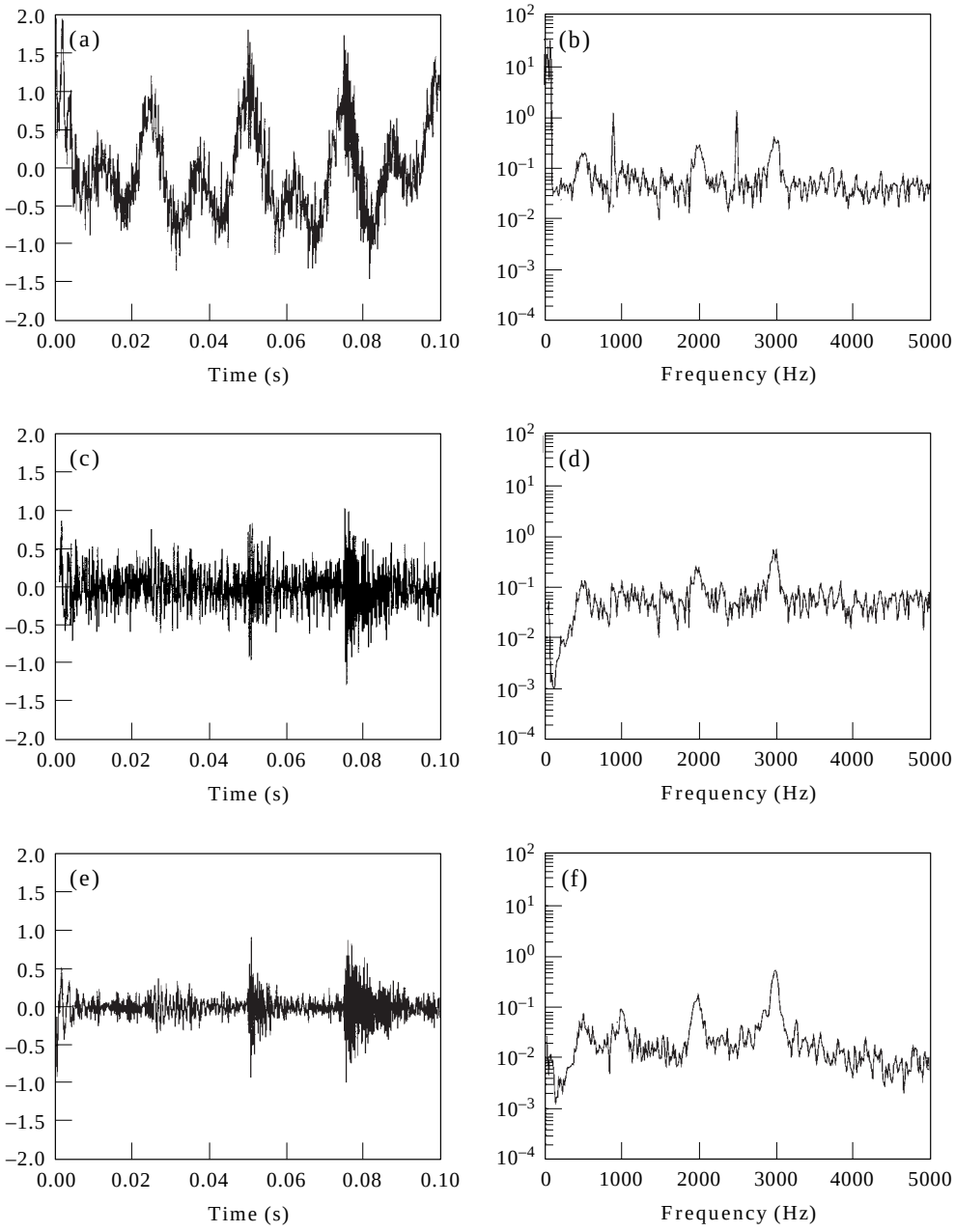

Figure 6. Enhancement of synthetic automotive engine data. (a) Synthetic data; (b) Fourier transform of synthetic data; (c) error output ($\varepsilon_{k,1}$) from the first stage; (d) Fourier transform of $\varepsilon_{k,1}$; (e) filter output ($y_{k,2}$) from the second stage; (f) Fourier transform of $y_{k,2}$.

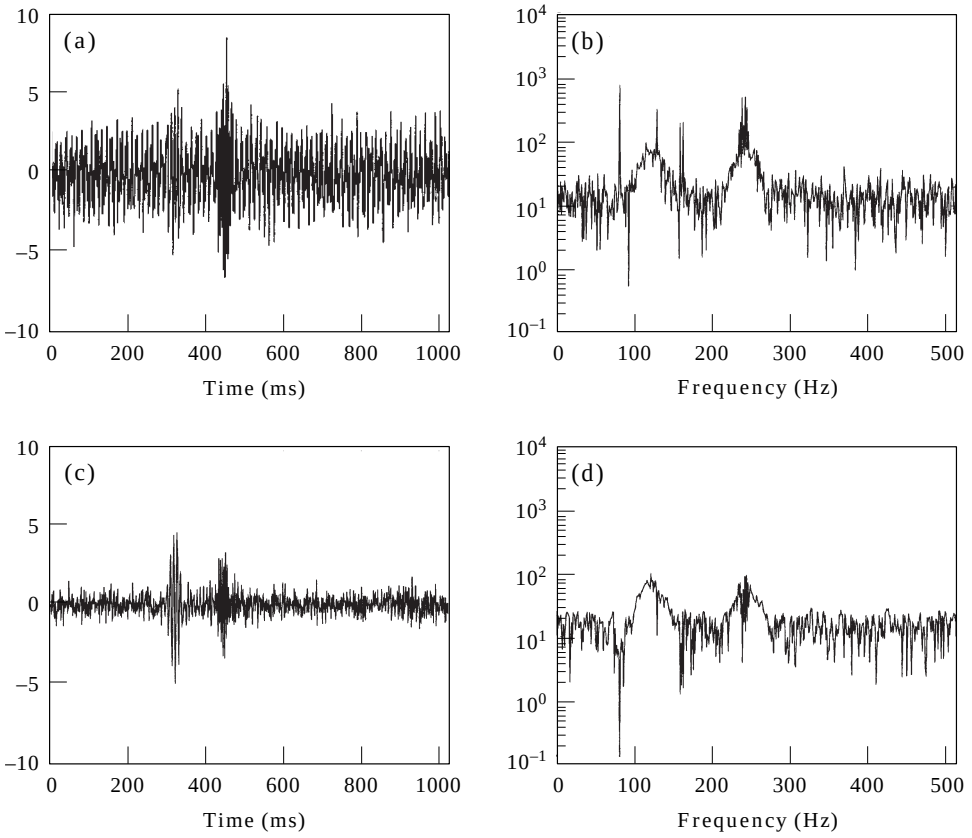

Figure 7. Enhancement of synthetic gearbox data. (a) Synthesized data; (b) Fourier transform of synthesized data; (c) error output ($\varepsilon_{k,1}$) from the first stage; (d) Fourier transform of $\varepsilon_{k,1}$.

unprocessed time series, Figure 6(a), and in its Fourier transform, Figure 6(b). In the output of the first stage, shown in Figures 6(c) and (d), the narrowband components have been significantly attenuated. The impulsive signals are more clearly evident in the time series, Figure 6(c), but are still significantly masked by the broadband noise. Applying the second adaptive filtering stage reduces the level of this noise, leaving a much clearer time series, Figure 6(e), and Fourier transform, Figure 6(f).

Figure 7 shows the result of applying ALE to the synthetic gearbox data. In general, the level of broadband noise in gear vibration data is lower than that observed in the engine data sets, and this is reflected in our simulated signals. The result is that, generally, it is sufficient to only apply the first stage of the scheme, i.e., to attenuate the narrowband components. In the original time series, and its Fourier transform, Figures 7(a) and (b) respectively, the impulsive signals are effectively masked.

The impulsive components are not easy to discern in the unprocessed time series as shown in Figure 7(a) nor in their Fourier transform Figure 7(b). The output of the first stage is shown in Figure 7(c), where the narrowband components, both

at low and mid frequencies, have been significantly attenuated, with the result that the impulsive signals are clearly evident, negating the need to apply the second adaptive filtering stage. Further in the Fourier transform, Figure 7(d), the contributions of the impulsive components are clearly evident as broad peaks about 128 and 265 Hz.

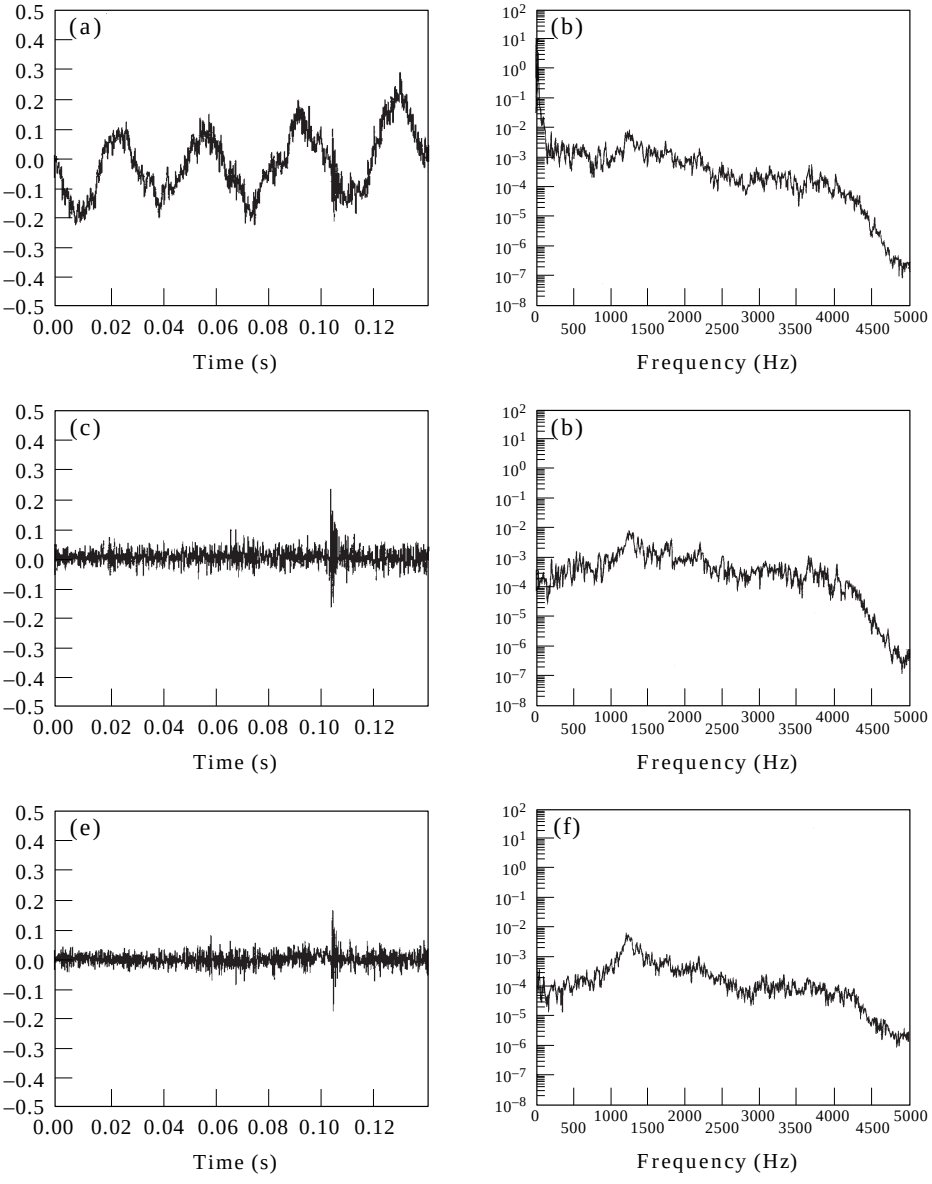

Figure 8. Results of enhancement for measured data from an automotive engine. (a) Time series data; (b) Fourier transform of data; (c) error output ($\varepsilon_{k,1}$) from first stage; (d) Fourier transform of $\varepsilon_{k,1}$; (e) Filter output ($y_{k,2}$) from the second stage; (f) Fourier transform of $y_{k,2}$.

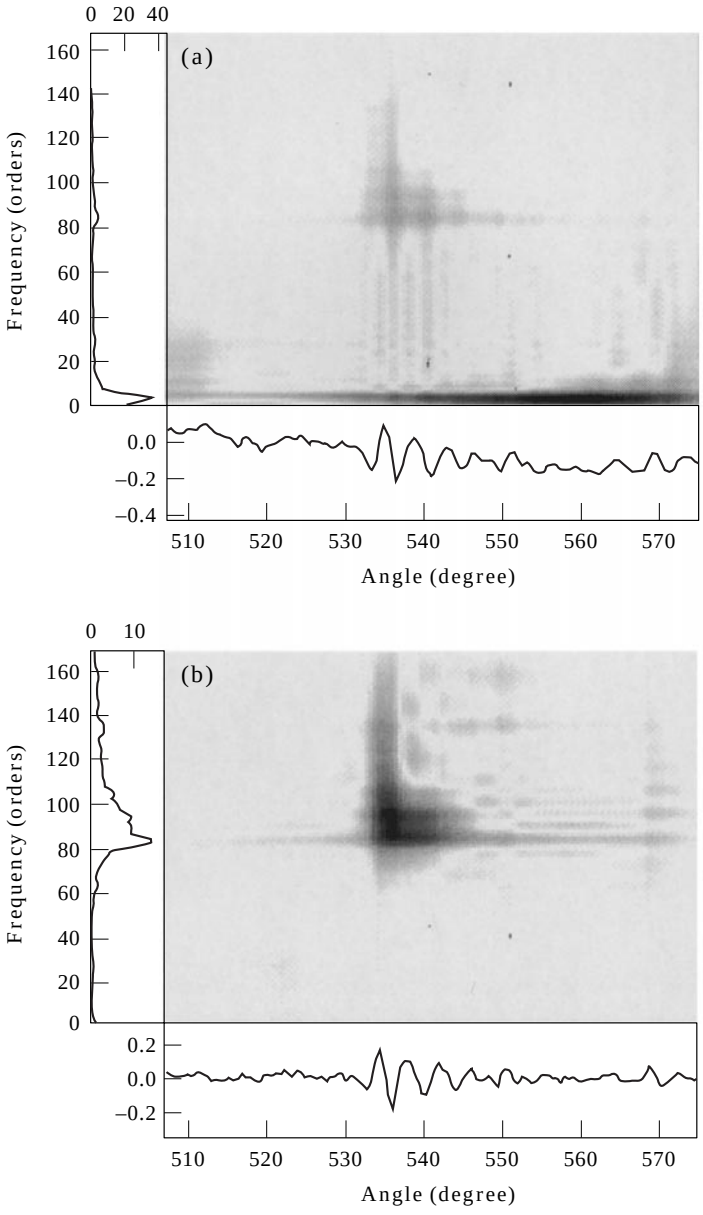

Figure 9. Time–frequency analysis of automotive engine data. (a) Choi–Williams distribution of raw data; (b) Choi–Williams distribution of enhanced data.

5. APPLICATION TO MEASURED DATA SETS

5.1. AUTOMOTIVE ENGINE DATA

The vehicle used in this test is a European passenger car with a 2·0 litre, in-line, 4 cylinder engine. This engine has no fuel injection system. The engine was operating at a nominal idling speed of 890 rpm: i.e., one order is approximately 14·8 Hz. The impulsive sounds are introduced by loosening a spark plug.

One microphone was used to make a measurement in the engine compartment. This microphone was calibrated using a Brüel and Kjaer pistonphone [94 dB(A)]. The measured analogue data were converted to digital form at a sampling rate of 10 kHz.

Figure 8 shows the signal after enhancement by the two-stage ALE. After the first stage ALE the harmonic noises at engine rotation speed and pure tone noises are nearly cancelled, as shown in Figures 8(c) and (d). The impulsive sound is further enhanced via the second stage ALE, the output of which is shown in Figures 8(e) and (f). Visually the success of the second stage can be seen, since the level of the broadband noise has been reduced. From examination of the Fourier representation, Figure 8(f), it can be seen that the impulsive sound of the test car engine has a peak at slightly less than 1·3 kHz. This impulsive sound is non-stationary in nature and one cannot readily use the frequency domain representation to identify the temporal location of an event. This is important since the location in time of an event gives information about the cause of the fault.

Figures 9(a) and (b) show the Choi–Williams distributions of the raw and enhanced data, respectively. Form Figure 9(a) the impulsive signals are effectively masked by the background noise. Whilst Figure 9(b) is clearer and one can identify

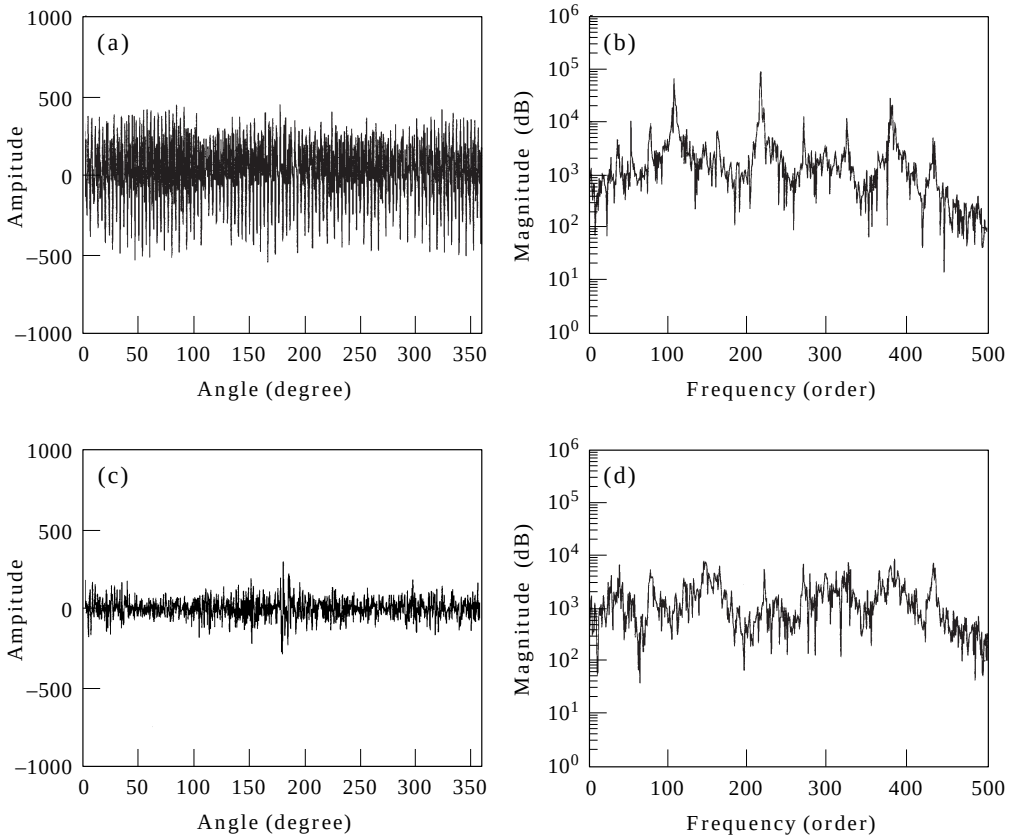

Figure 10. Results of enhancement for measured data from a gearbox. (a) Time series data; (b) Fourier transform of data; (c) error output ($\varepsilon_{k,1}$) from first stage; (d) Fourier transform of $\varepsilon_{k,1}$.

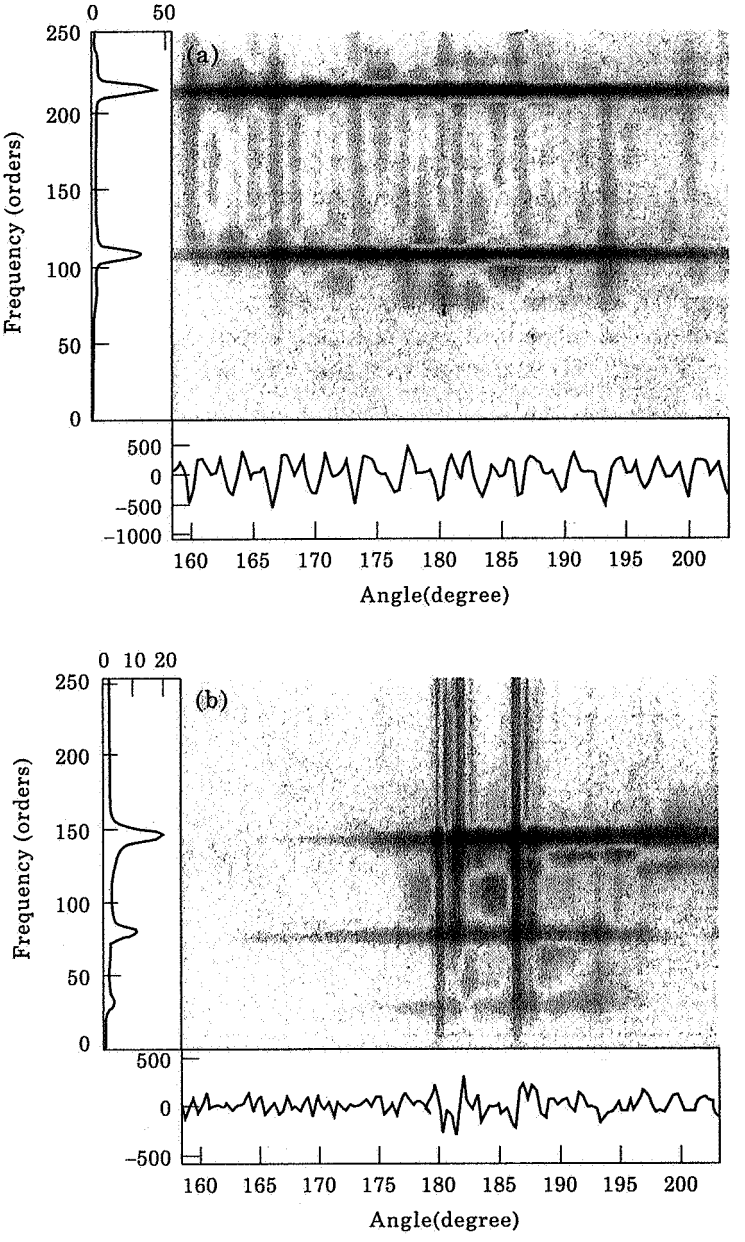

Figure 11. Time–frequency analysis of gearbox data. (a) Choi–Williams distribution of raw data; (b) Choi–Williams distribution of enhanced data.

that the impulsive signal is associated with a crankshaft angle of roughly 530° and a centre frequency of the 85th order (12·6 kHz), the picture is still partially obscured by obtrusive cross-terms.

5.2. GEARBOX DATA

A great deal of research into the early detection of faults in gears has been undertaken [8, 30]. Figure 10(a) shows the vibration signal measured on the casing

of a gearbox in which a faulty gear is known to be present [30]. Figure 10(b) shows the Fourier transform of this data. From Figure 10(a) it is difficult to see the impulsive signal because of the large amplitude tonal signals which constitute the regular signal. In this gear the pinion has 28 teeth and the wheel has 55. Thus the 55th order represents the fundamental frequency. In order to remove the tonal signals of the tooth meshing frequency a two-stage ALE is employed. The residual component, $x_r(t)$, comes up clearly, as shown in Figure 10(c). Figure 10(d) shows the Fourier transforms of these signals.

Finally, if one uses the Choi–Williams distribution on the raw data, as shown in Figure 11(a), the result is relatively cross-term free. However, the fact that the regular signal is much larger than the impulsive signal means the contribution of the impulsive terms remain hidden. By first pre-processing the signal and then applying the Choi–Williams algorithm, Figure 11(b) is obtained in which the effect of the impulsive signal can be seen. From this final result one can conclude that the gear fault occurs at shaft angles of 180° and 186° and at 110 ± 28 orders of shaft rotating speed. This appears to result from an increase in the sidebands of the second meshing frequency of the wheel gear.

6. CONCLUSIONS

The impulsive sound and vibration signals in rotating machinery are useful indicators of faults in machinery. However the detection of these impulsive signals can be difficult due to the competing noise sources. Under circumstances when a synchronizing signal is unavailable an enhancement scheme, called the two-stage Adaptive Line Enhancer, has been presented. This comprises two ALEs each with a different role; one to remove tonal noise and the other to reduce broadband noise. This technique has been shown to perform effectively. It should be emphasized that whilst the performance of this system is encouraging, it is not claimed that its performance is better than that which can be achieved by the use of temporal averaging with a good reference signal. The utility of the method described here predominantly lies in those applications where a synchronous signal is unavailable, or is unreliable. This approach does have one further advantage over time averaging in that it will remove all tonal components from the data set, whereas temporal averaging can leave components which then need further processing to suppress them.

The power of this method was demonstrated on both synthetic signals and signals gathered from real machines. In both cases the success of the algorithm was visible in both the time and frequency domains and allowed successful characterization via a time–frequency representation.

ACKNOWLEDGMENT

The authors gratefully acknowledge the help of A. Rivola for supplying the gear vibration data relative from tests performed in the Department of Mechanical Engineering (DIEM) of the University of Bologna, Italy.

REFERENCES

1. S. G. Braun 1986 *Mechanical Signature Analysis—Theory and Applications*. New York: Academic Press.
2. P. D. McFadden 1987 *Mechanical Systems and Signal Processing* **1**(2), 177–183. Examination of a technique for the early detection of failure in gears by signal processing of the time domain average of the meshing vibration.
3. P. D. McFadden 1986 *Transactions of the ASME Journal of Vibration, Acoustics, Stress and Reliability and Design* **108**(2), 165–170. Detection fatigue cracks in gears by amplitude and phase demodulation of the meshing vibration.
4. R. Randall 1982 *Transactions of the ASME Journal of Mechanical Design* **104**(2), 259–267. A new method of modeling gear faults.
5. Q. Zhuge 1990 *Mechanical Systems and Signal Processing* **4**(5), 355–365. Non-stationary modelling of vibration signals for monitoring the condition of machinery.
6. D. Dyer and R. M. Stewart 1978 *Transactions of the ASME Journal of Mechanical Design* **100**(2), 229–235. Detection of rolling element bearing damage by statistical vibration analysis.
7. R. Randall 1981 *B & K Application Note, Technical Report*, 13–150. Cepstrum analysis and gearbox fault detection.
8. W. J. Wang and P. D. McFadden 1993 *Mechanical Systems and Signal Processing* **7**(3), 193–203. Early detection of gear failure by vibration analysis—I. Calculation of the time–frequency distribution.
9. W. J. Staszewski and G. R. Tomlinson 1997 *Mechanical Systems and Signal Processing* **11**, 331–350. Local tooth fault detection in gearboxes using a moving window procedure.
10. S. K. Lee and P. R. White 1997 *ASME Design Engineering Technical Conferences, 16th Biennial Conference on Mechanical Vibration and Noise*, DETC97/VIB-4236. Fault identification for rotating machinery using adaptive signal processing and time–frequency analysis.
11. A. M. Zoubi and J. F. Böhme 1995 in *Higher-Order Statistical Signal Processing* (editors B. Boashash *et al.*), 270–290. Application of higher-order spectra to the analysis and detection of knock in combustion engines. London: Longmans.
12. S. K. Lee and P. R. White 1997 *Mechanical Systems and Signal Processing* **11**(4), 637–650. Fault diagnosis of rotating machinery using Wigner higher order moment spectra.
13. R. M. Stewart 1977 *ISVR, University of Southampton, Report MHM/R*/10/77. Some useful data analysis techniques for gearbox diagnostics.
14. S. G. Braun and B. B. Seth 1979 *Journal of Sound and Vibration* **65**(1), 37–50. On the extraction and filtering of signals acquired from rotating machines.
15. P. D. McFadden 1989 *Mechanical Systems and Signal Processing* **3**(1), 87–89. Interpolation techniques for time domain averaging of gear vibration.
16. P. D. McFadden 1987 *Mechanical Systems and Signal Processing* **1**(1), 83–95. A revised model for the extraction of periodic waveforms by time domain averaging.
17. G. Chaturvedi 1981 *Journal of Sound and Vibration* **76**(3), 391–405. Adaptive noise cancelling and condition monitoring.
18. S. K. Lee and P. R. White 1996 *IEE Colloquium on Modelling and Signal Processing for Fault Diagnosis*, Ref. No. 1996/260, 1/6–6/6. Fault diagnosis of rotating machinery using a two-stage adaptive line enhancer.
19. B. Widrow and S. D. Sterns 1985 *Adaptive Signal Processing*. Englewood Cliffs, NJ: Prentice-Hall, first edition.
20. J. R. Zeidler, E. H. Satorius, D. M. Chabries and H. T. Wexler 1978 *IEEE Transactions on Acoustics, Speech and Signal Processing* **26**, 240–254. Adaptive enhancement of multiple sinusoids in uncorrelated noise.

21. B. Friedlander 1982 *Proceedings of the IEEE* **70**(8), 829–867. Lattice filters for adaptive processing.
22. S. Haykin 1991 *Adaptive Filter Theory*. Englewood Cliffs, NJ: Prentice-Hall, second edition.
23. I. K. Proudler and J. G. McWhirter 1992 *RSRE Memorandum No*. 4562; RSRE Malvern, Worcs., U.K. QR decomposition based algorithms and architectures for least-squares adaptive filtering.
24. L. Cohen 1996 *Journal of Mathematical Physics* **7**(5), 785–788. Generalised phase–space distributions.
25. H. I. Choi and W. Williams 1989 *IEEE Transactions* **37**, 862–971. Improved time–frequency representation of multiple component signals using an exponential kernel.
26. S. K. Lee, S. D. Yeo, B. J. Kim and I. H. Rho 1994 *Society of Automotive Engineering*, SAE 940995. Weight reduction and noise refinement of 1·5 litre engine.
27. S. K. Lee and P. R. White 1997 *Proceedings of the* 1997 *Noise & Vibration Conference SAE*, SAE 970262. Impulsive sound analysis of automotive engine.
28. P. R. White 1992 *Ph.D. Thesis*, *ISVR*, *University of Southampton*. Adaptive signal processing and its application to infrared detector systems.
29. J. A. Cadzow 1983 *Proceedings of the IEEE*, **130**(3), 202–210. Singular-value decomposition approach to time series modelling.
30. G. Dalpiaz, A. Rivola and R. Rubini 1996 *Proceedings of the Congress of Technical Diagnostics—KDT* '96, *Gdansk*, *Poland*, 185–192. Dynamically modelling a gear system for condition monitoring and diagnostics.